

A Study of the Swelling and Bursting of the High Pressure Coupling (HPC) of a Two-Stage Light Gas Gun

David W. Bogdanoff

Senior Research Scientist, Analytical Mechanics Associates, Inc., Moffett Field, CA 94035

Abstract

A consistent picture of the swelling and bursting of the high pressure couplings (HPC) of two NASA Ames two-stage light gas guns is developed. The following information is used to construct the model.

1. Experimental measurements of the swelling and bursting of the HPCs of two two-stage light gas guns.
2. Stress-strain calculations of the swelling and bursting of thick walled steel tubes.
3. Experimental measurements swelling and bursting of thick walled steel tubes.
4. CFD calculations of the maximum pressures in the HPC of a two-stage light gas gun using the code LGGUN

It is suggested that the techniques described herein could be used to assess the likelihood of swelling and bursting of the HPCs of various different two stage light gas guns.

1. Introduction

NASA needs to understand the hypersonic flight characteristics of earth and planetary entry vehicles and the amount of damage that can occur due to hypervelocity impact of space debris and naturally occurring meteoroids. Investigations of this sort can involve test articles that are launched at velocities of ~ 7 km/s or more. Such launches can aid in evaluating new (or existing) designs for earth and planetary entry vehicles, vehicle static and dynamic stability and aerodynamic heating response.

The two-stage light gas gun is a well-known method of achieving such high velocity launches. Figure 1 below shows a schematic sketch of a two-stage light gas gun.

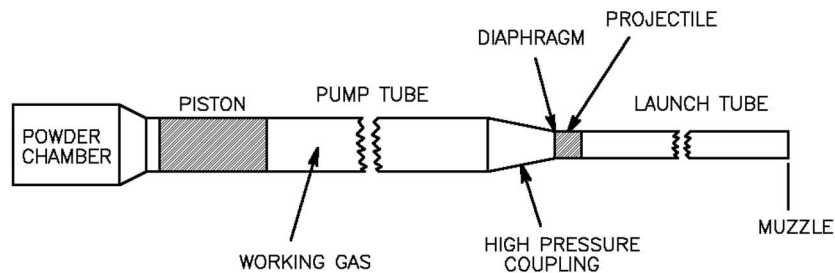


Figure 1. Schematic sketch of a two-stage light gas gun.

The gun comprises:

- Powder chamber
- Pump tube with piston
- High pressure coupling cone
- Rupture diaphragm
- Launch tube with projectile

Figure 2 shows some of the details of the high pressure coupling (HPC).

The gun operation cycle is as follows:

- Powder burns, accelerates piston
- Piston compresses working gas to very high pressure and temperature
- Diaphragm breaks
- High pressure, high temperature gas accelerates projectile down launch tube

2. Danger of swelling and bursting of HPC; calculated and measured maximum pressures

The piston is brought to a halt in the conical section of the high pressure coupling (HPC). The highest pressures occur in this section. For high performance shots (muzzle velocities above 7 - 8 km/s), swelling and bursting of the HPC can be serious problems. It would be extremely useful to know how to set the gun operating conditions so as to limit HPC swelling and avoid bursting the HPC. In this report, we attempt to do so by correlating experimental swelling and bursting data with gun operating conditions and with CFD predictions of maximum gun pressures. The guns involved for this study are the NASA Ames 0.28"/1.55" and 0.50"/2.50" guns. (The first number indicates the launch tube diameter and the second number is the pump tube diameter.) The gun operating conditions, gun performances (i.e., piston and projectile velocities) and HPC swelling and bursting data were gathered from the facility log book "Gun Dev" (Ref. 1). The entries in Ref. 1 date from 12/8/64 to 10/13/70.

Maximum measured projectile base pressures are found in Ref. 2 (AGARDograph 138), Figs. 2.46 and 2.47, pp. 77 and 78. Maximum projectile base pressures and maximum gun pressures were calculated using the CFD code LGGUN. A description of the LGGUN code and its validation is given in Appendix A. For 14 shots on the Ames 0.28"/1.55" gun and 1 shot on the Ames 0.50"/2.50" gun, Fig. 3 gives the maximum gun pressures calculated versus the muzzle velocity for the shot. It can be seen that there is a large increase in the maximum gun pressure as one moves from the muzzle velocity range of 7 - 8 km/s to the range of 9 - 10 km/s. (Numbers next to data points are the per shot swelling measurement, in thousandths of an inch, of the HPC diameter. The original diameter was 7.75".) For two of the highest velocity points, a substantial HPC swelling and a HPC burst occurred.

3. Comparison of experimental maximum projectile base pressures with those calculated using the CFD code LGGUN

A comparison is made in Fig. 5 between experimental measurements [made using a microwave technique (Ref. 3)], plotted on the x-axis, and the CFD values (calculated using the LGGUN code), plotted along the y-axis. It is seen that the experimental and CFD values agree to within $\pm 20\%$ for about 60% of the data points and within $\pm 40\%$ for the remainder of the data points. This level of agreement, maintained over an order of magnitude change of the variable values, was deemed to be acceptable and is taken as an additional validation of the LGGUN code.

4. Experimental data on the bursting pressures of heavy walled steel cylinders

References 4 and 5 present experimental data on the bursting pressures of heavy walled steel cylinders. Data is presented for wall diameter ratios (R = outside diameter divided by inside diameter) of 1.2 to 8.0. The data are found to correlate well with the equation

$$p_b = 1.155\sigma_y(\ln R) \left(2 - \frac{\sigma_y}{\sigma_u}\right) \quad (1)$$

where:

- p_b = burst pressure
- σ_y = 0.20% tensile yield stress
- σ_u = ultimate tensile stress
- R = wall diameter ratio (outside/inside)

The data from Refs. 4 and 5 was scaled starting with σ_y and σ_u from the references and scaling up to σ_y (= 140 ksi) and σ_u for the 4340 steel of the Ames guns. This scaled data is shown by the data points of Fig. 5. Figure 5 also shows the plot of the burst pressure of a thick walled tube based on the elastic-perfectly plastic solution of the stress-strain equations with σ_y = 140 ksi. References 6 and 7 present the development of this burst pressure equation and Ref. 7 shows that the equation is valid for diameter ratios less than about 6. Also shown is the logarithmic fit to the data of Refs. 4 and 5, equation 1, which reduces to $p_b = 172 \ln R$. Figure 6 repeats Fig. 5 with the addition of 5 new (blue) data points from shots on the Ames 0.28"/1.55" gun and two new trend lines (red and blue). The data points are calculated maximum pressures in the high pressure coupling (HPC) versus tube diameter ratio at the location of the maximum pressure. The calculations were done using the code LGGUN. The red trend line is taken from Ref. 8 with σ_y = 140 ksi. The authors of Ref. 8 first developed a theoretical model

for the tube stresses and strains and then showed that their solution for the burst pressure matched within 2% with the empirical expression $p_b = 1.08\sigma_y \ln R$ derived from experimental data. The blue trend line is based on results of Ref. 8a. The authors of Ref. 8a developed a model where the tube stress-strain relations are related to experimental stress-strain relations obtained from tension (or torsion) tests. Thus, the blue trend line is based on experimental stress-strain relationships (for a differing geometry), while the red trend line is not. The blue trend line was constructed by starting with the solution given in Tables 5 and 7 of the reference which is for Vibrac steel at diameter ratios (R) of 1 to 10. The burst pressures for the solution of the reference were then multiplied by the ratio of the ultimate stresses of the 4340 steel of the NASA gun (150 ksi) to that for the Vibrac steel of the reference (122 ksi). It is seen that the red and blue trend lines are very close to each other and thus the blue line offers additional confidence for the red line up to $R = 10$. Since the HPC survived the shots yielding the new (blue) data points, it is assumed that we may extend the red burst pressure trend line to $R = 17$. However, we shall use the more conservative green trend line in subsequent evaluations of the risk of bursting of the HPC, which incorporates an additional 8% factor of safety.

5. Representative key outputs from runs of the CFD code LGGUN

Sixteen LGGUN CFD code runs were made for shots using the Ames 0.28"/1.55" two-stage light gas gun. Figure 7 shows key outputs from the run simulating shot 156. This was a moderate energy (33 g of gunpowder) shot. The data are mainly presented in the form of a snapshot taken at the time of maximum pressure in the gun. The abscissa (x) is the distance along the gun from the blind end of the powder breech towards the gun muzzle. The region shown in Fig. 7 covers the most down range 20 cm of the "pump tube" (actually the uprange cylindrical bore of the HPC) the HPC conical section and the most up range 30 cm of the launch tube. The entire piston is captured within the HPC for this particular snapshot. The variables plotted are:

- Piston position at time of snapshot (black vertical dashed lines)
 - Snapshot pressure (solid red line)
 - Tube outside/inside area ratio (blue line)
 - Tube burst pressures calculated using the method from Refs. 6 and 7 described in Sec. 4 and taking $\sigma_y = 140$ ksi (green line)
- (The plots of the 4 variables listed above are all valid at snapshot time - the plots of the 2 variables listed below are not snapshots)
- Maximum pressures at each x location (dashed red line)
 - The piston front velocity versus x (purple line)

Figure 8 shows corresponding CFD outputs for shot 83 on the same gun. This was a higher energy (40 g of gunpowder, 8.7 km/s muzzle velocity) shot. Figure 9 shows corresponding CFD outputs for shot 166. This was a still higher energy (42

g of gunpowder, 9.3 km/s muzzle velocity) shot. Figure 10 shows corresponding CFD outputs for shot 196. Note that the nominal gun firing conditions for shot 196 are essentially the same as those for shots 195 and 197, except for the loading position of the projectile down the barrel, which varies from 10 to 30 cm. These were moderate energy (39 g of gunpowder, 8.3 - 8.8 km/s muzzle velocity) shots, except for shot 197, where the projectile was loaded very far forward (by 30 cm) in the launch tube and the resulting muzzle velocity was only 5.3 km/s. For shot 196 (and for all of shots 180 to 202), the pump tube length was shortened by a factor of 2.

The results for the series of CFD runs for shots on the 0.28"/1.55" gun can be broadly divided into two groups, for which Figs. 7 and 9 are representative. Figure 11 shows CFD outputs for shot 33-93 on the Ames 0.50"/2.50" gun. This was a very high energy [48 g of gunpowder (scaled to smaller gun), 10.2 km/s muzzle velocity (calculated)] shot. The HPC burst on this shot. This run would clearly belong in the high energy grouping of the runs for the 0.28"/1.55" gun. Unfortunately, the piston front velocity trace was not available for this run. CFD calculations were also done for shot 22-82 on the Ames 0.50"/2.50" gun. This was a moderately high energy 39 g of gunpowder (scaled to smaller gun), 9.4 km/s muzzle velocity shot.

For both classes of shots for the 0.28"/1.55" gun, the piston front starts to accelerate upon entering the cone. For the lower energy shots, the piston front velocity peaks out, starts to decrease in the cone and finally, the piston front comes to a halt in the cone. For the higher energy shots, the piston front acceleration slows down about 80% of the way through the cone and then increases strongly in the last 20% of the travel through the cone. The piston front then continues into the launch tube and finally, comes to a halt 5 to 20 cm down range from the end of the cone. Extrusion of piston material into the launch tube has been observed experimentally for high energy shots. For the 0.28"/1.55" gun, piston material was observed in the launch tube after shots 195 and 196. After a shot on the NASA Ames 1.0"/4.0" gun, a 6" long slug of piston material was found in the launch tube.

Maximum pressures are observed in the most down range 30 - 50% of the cone length where the flow is most contracted. In many cases, at the time of maximum pressures, the front of the piston is located in the region of maximum pressures. The pressures drop 30 - 50% as one leaves the cone and passes in to the launch tube size bore. Pressures in the down range 30 - 50% of the cone are predicted to be very high. Of the 20 cases studied in detail, 13 had maximum pressures of up to 300 ksi, 4 had maximum pressures of 300 - 430 ksi and three had maximum pressures of 458, 652 and 814 ksi. For the 458 ksi case, the HPC survived but no swelling measurements were made. For the 652 ksi case, the HPC swelled 0.015" on the diameter but did not burst. For the 814 ksi case, the HPC burst.

Figure 12 shows the maximum gun pressures calculated using LGGUN for these 20 cases plotted against the HPC outside/inside diameter ratio where the maximum pressure occurs. Also shown are the experimental data^{4,5} on bursting pressures material scaled to the material of the Ames guns. The lower energy shots are typified by shot 156, for which we see, from Figs. 7 and 12, the burst

pressure estimate exceeds the maximum pressure calculated using LGGUN by 20%. The higher energy shots are typified by shots 166 and 33-93 (on the 0.50"/2.50" gun), for which we see from Figs. 9, 11 and 12, the maximum pressure calculated using LGGUN exceeds the burst pressure estimates by 55 - 115%. Shot 83 is an intermediate energy shot, for which data is presented in Figs. 8 and 12. For this shot, the maximum pressure calculated using LGGUN is nearly equal (4% difference) to the calculated burst pressure.

Table 1 below summarizes key HPC peak pressures and burst pressures in the cone part of the HPC from figures 7 to 12. Column 2 is the outside/inside diameter ratio of the HPC at the point of maximum pressure predicted by LGGUN. Column 3 is that maximum predicted pressure. Column 4 is the calculated burst pressure. Column 5 is the prediction of the swelling and bursting of the cone part of the HPC based on the peak pressures and the burst pressures in the two previous columns. Column 6 gives the swelling and bursting presumed to have been observed in the 1.55" diameter part of the HPC. (The notes in the log book, from 1967, simply say, for example, "Coupling Grew .004".) Color coding goes with whether the predicted maximum pressure or the burst pressure is the larger and favorable or unfavorable outcome of the shot. Note that the entries in column 5 and 6 are at different and varying locations in the HPC and hence, there is no reason for them to track together closely, although they do track in a general way as one moves from low energy to high energy shots.

Table 1. Key HPC peak pressures and burst pressures in the cone part of the HPC from figures 7 to 12.

Shot #	Diameter ratio, R	Peak press	Burst press	Swell or burst prediction in cone part of HPC	Swell or burst observed in 1.55" diameter part of HPC
		ksi	ksi		in
156	11.8	290	346	Small	0.003
83	12	355	348	Borderline	0.001
166	21.5	660	430	Burst	0.015
33-93	14.5	812	374	Burst	Burst

Burst press = 140*LN(R)

6. Comparisons, in full pump tube inside diameter part of HPC of theoretical and experimental maximum pressures

For the cylindrical portion of the HPC at the full pump tube inside diameter (with R = 5 or 4.8), this section compares the maximum HPC pressures calculated from experimental swelling and bursting data with the LGGUN-predicted maximum pressures, Reference 9 presents a method of calculating the radial displacements of a heavy wall tube during autofrettage (application of pressure) and the subsequent release of pressure. At the maximum pressure, the inner part of the tube is taken to be perfectly plastic, with $\sigma_r - \sigma_t = \sigma_y$, where σ_r = radial stress, σ_t = tangential stress and σ_y = yield stress. The outer part of the tube is taken to be perfectly elastic. The displacements of the tube, as it is relaxed down to zero

applied pressure, are assumed to occur elastically. Reference 9 gives expressions for the final strains of the outer surface of the tube. Using these expressions, we can construct Table 2 relating the measured swelling or bursting of the HPC to the maximum pressure undergone during the previous gun firing.

Table 2. Relation between observed HPC swelling or bursting and maximum pressures undergone in the uprange cylindrical part of the HPC.

Gun	Swelling on diameter	Maximum pressure based on swelling or bursting
	inches	ksi
0.28"/1.55"	0.001	132
0.28"/1.55"	0.002	146
0.28"/1.55"	0.003	160
0.28"/1.55"	0.004	170
0.28"/1.55"	0.005	180
0.28"/1.55"	0.015	220
0.50"/2.50"	Burst	220

Figure 13 shows the maximum HPC pressures in the upstream cylindrical section calculated from HPC swelling and burst (from Table 2) vs those calculated with LGGUN. It is seen that, with exception of one "rogue point", the agreement is quite good. (The red data point will be discussed at a later point in this report.) Disagreements between theory and experiment are less than 10% for 4 out of 9 points with 2 additional data points with disagreements of ~20% and 2 more additional data points with disagreements of ~30%. Since the maximum HPC pressures based on swelling and burst are completely independent of those calculated using LGGUN, this degree of agreement offers further validation of the LGGUN code.

The data of Fig. 13 can be replotted as shown in Fig. 14, emphasizing swelling and bursting as results of the ratio (R_p) of the maximum HPC pressure in the upstream cylindrical section of the HPC divided by the burst pressure for same. Figure 14 shows the swelling and bursting in the upstream cylindrical section of the of HPC plotted versus the pressure ratio R_p . There are more data points in Fig. 14 than in Fig. 13 and for some of the data points with zero swelling shown there may have been swelling, without it having been noted down in the log book. From Fig. 14 the following observations may be made:

1. $R_p = 0.0 - 0.50$, no swelling (except at rogue point)
2. $R_p = 0.5 - 0.77$, red curve passes close to 4 points, but pressure ratios at growths of ~0.005" are 30% low, growths of 0.0 - 0.005"
3. $R_p = 0.77 - 1.10$, steep rise in growth (0.004 - 0.015") terminating in bursting. Red curve passes (about midway) between the point with 0.015" swelling and the point with HPC burst, as it should.

Figures 13 and 14 may be used, together with the LGGUN calculations, to assess the likelihood of swelling and bursting at the full pump tube inside diameter part of the HPC. Table 3 below gives key HPC peak pressures and burst pressures in the 1.55" diameter part of the HPC and corresponds to Table 1, which is for the cone part of the HPC. In Table 3, columns 5 and 6 are for the same location in the HPC and hence the numbers in these columns track fairly closely. Note from Fig. 14 that, for shot 166, a change in pressure of only 12% would bring the predicted and observed swellings into agreement.

Table 3. Key HPC peak pressures and burst pressures in the 1.55" diameter part of the HPC from figures 7 to 12.

Shot #	Diameter ratio, R	Peak press ksi	Burst press ksi	Swell or burst prediction in 1.55" diameter part of HPC in	Swell or burst observed in 1.55" diameter part of HPC in
156	5	158	225	0.0025	0.003
83	5	131	225	0.001	0.001
166	5	186	225	0.0057	0.015
33-93	4.8	247	220	Burst	Burst

Burst press = 140*LN(R)

Note from Figs. 7 to 11, there are two locations in the HPC where the margins between the peak pressure and the burst pressure are the smallest for that part of the HPC. One is at the absolute maximum pressure in the HPC (for cone part of HPC) and the second is at the downrange end of the full pump tube inside diameter part of the HPC (for 1.55" or 2.5" inside diameter part of HPC). This is also true for the other 16 shots for which these types of plots were made. It is presumed that if the pressure margins at these locations are found to be acceptable that the design of the whole HPC is acceptable regarding wall thickness. The analyses at these two locations were discussed in sections 5 and 6.

From Tables 1 and 3 above,

1. For shot 156, the predictions for swelling are "small" (Table 1) and 0.0025" (Table 3) and the observed swelling was 0.003" (Table 3).
2. For shot 83, the predictions for swelling are "borderline" (Table 1) and 0.001" (Table 3) and the observed swelling was 0.001" (Table 3).
3. For shot 166, the predictions for swelling are "burst" (Table 1) and 0.0057" (Table 3) and the observed swelling was 0.015" (Table 3).
4. For shot 33-93, the predictions for swelling are "burst" (Table 1) and "burst" (Table 3) and the observed swelling was "burst" (Table 3).

For the first and fourth cases above, the predictions and observations correspond. For shot 83, the prediction for the swelling of the full pump tube diameter part of the HPC corresponds to the observation, but the prediction for the

swelling in the cone is not "small", but "borderline". However, as mentioned previously, the location of the cone prediction is not at the full pump tube inside diameter point of observation. For shot 166, the prediction of swelling from the cone pressures is "burst" and that from of the full pump tube diameter part of the HPC is 0.0057". The observation is 0.015". Thus, although the HPC did not burst, it underwent a large growth. Note that, in this case also, the locations do not correspond.

7. Comparisons of theoretical and experimental maximum pressures in 0.300" inside bore diameter part of the HPC

At the beginning of the previous section we have given a theoretical method for the prediction of the swelling of the outside diameter of the HPC using the elastic-plastic model, wherein the outer part of the HPC is taken to behave elastically and the inner part of the HPC is assumed to behave in a perfectly plastic manner. We obtain the swelling of the inner bore at the small end of the HPC as follows. We define

- a = radius of inner bore of small end of HPC
- b = outer radius of HPC
- c = radius of HPC at elastic-plastic transition

Figure 15 shows the various radii and the elastic and plastic zones of the HPC. We have the swelling at radius b. Using the equations of Ref. 9a, the swelling at radius c can be calculated. Using Eq. (24) of Ref. 8a, p. 108 and the assumption of the reference that the total volume of the material in the plastic part of the HPC remains unchanged during the swelling, we can calculate the swelling at radius a and the corresponding maximum pressure undergone. These can then be compared with CFD calculated maximum pressures. The comparison can be made in Fig. 10. (For more details, see Appendix B.) The CFD maximum pressures range from 9 to 13 x 10⁹ dynes/cm², the average being 11 x 10⁹ dynes/cm². The maximum pressure based on swelling is 17 x 10⁹ dynes/cm². Thus, the CFD maximum pressure predictions underpredict the maximum pressure derived from the experimental swelling data by 35%. This data point is plotted in red in Fig. 14. We note that its underprediction is slightly worse than the worst blue data point of Fig. 14, with the exception of the "rogue" point. For the poorest non-rogue blue data point, the underprediction is 30.5%. We deem the 35% difference acceptable.

8. Conclusions

From the preceding sections and Appendices A and B, a consistent picture of the swelling and bursting of the high pressure couplings (HPC) of two Ames two-

stage light gas guns has been developed. The following information was used to construct the model:

1. Experimental measurements of the swelling and bursting of the HPCs of two two-stage light gas guns.
2. Stress-strain calculations of the swelling and bursting of thick walled steel tubes.
3. Experimental measurements swelling and bursting of thick walled steel tubes.
4. CFD calculations of the maximum pressures in the HPC of a two-stage light gas gun using the code LGGUN

It is suggested that the techniques described herein could be used to assess the likelihood of swelling and bursting of the HPC of various different two stage light gas guns. If such were to be done, the steps involved would be:

1. Construct a model of the new gun geometry (as in Fig. 1 with all dimensions specified).
2. Choose gun operating conditions -
 - a. Powder load
 - b. Hydrogen pressure
 - c. Piston mass
 - d. Break valve rupture pressure
 - e. Projectile mass
3. A good start on the items in 1 and 2 above can be found in Ref. 10 (Note that the 0.28"/1.55" gun discussed in the present report is the same gun for which much data is given in reference 10.)
4. Perform LGGUN calculations leading to results like Figs. 7 to 10 in the present report.
5. Pick off the absolute maximum HPC pressure and the maximum HPC pressure in the full pump tube inside diameter part of the HPC.
6. If the HPC material is closely comparable to the 4340 steel (yield stress = 140 ksi) of the Ames guns, Figs. 12 and 14 of the present report can then be used to assess the risk of swelling and bursting of the new HPC.
7. If the HPC is monobloc and steel, with Young's modulus 30 Msi and Poisson's ratio of 0.3, the analyses leading to Figs. 12 and 14 remain valid if the burst pressures are scaled with the yield stress. With this scaling, Figs. 12 and 14 of the present report can still be used to assess the risk of swelling and bursting of the new HPC.
8. If the HPC is radically different from those discussed herein, new calculations will have to be made to produce plots which correspond to those in Figs. 12 and 14 to assess the likelihood of swelling and bursting of the new HPC.

Appendix A - LGGUN code

A1. Introduction

LGGUN is a quasi-one-dimensional Godunov code¹¹ which is second order accurate in time and third order accurate in space, uses realistic equations of state for all media, includes wall friction and heat transfer for all gas and dense media zones and includes a simple non-equilibrium model for gas phase turbulence. The entire gun is divided into cells by a number of planes normal to the gun axis. Gun tube wall heating, melting/ablation and the incorporation of melted wall material (taken to be fine droplets) into the (usually) hydrogen working gas is modelled. It has been extensively validated against analytical solutions and experimental firing data from two stage guns at the NASA Ames and Marshall Research Centers operated over a wide range of operating conditions with muzzle velocities of 0.7 to 11.3 km/s. The code is written in Fortran and CPU times for a total of 138 active computational cells and ~12,500 time steps ranged from 35 to 570 s. The code outputs piston and projectile velocities, maximum gas pressures and temperatures at selected locations and cells, snapshots of conditions at specific times and a number of time history files at the projectile base, and at user-selected positions along the gun and for user-selected cells. Also given are the maximum gun tube wall and internal temperatures and the profile along the gun of the depth of eroded (melted) wall material during the shot.

A2. Code Description

The code is described in considerable detail in Refs. 11 and 12, but is also outlined here. It is a Godunov code, which means that at every time step, at every cell boundary, a Riemann problem is solved in order to obtain the cell boundary fluxes. The Riemann solvers used are very nearly exact. The code is third order accurate in space and uses the MacCormack predictor-corrector scheme,¹³ which is second order accurate in time, to advance in time. Most of the time, three different zones are used, each filled with a different media: (1) gunpowder/powder gas, (2) the pump tube piston and (3) the gun working gas plus melted droplets from the gun tube walls. When a plastic piston is weighted with a metal slug in the rear, four zones are used with the piston made up of two zones, metal aft and plastic forward. Gun working gases H₂, He, N₂ and Ar have been modelled. The projectile is not subdivided into zones, but is treated as a point mass, dynamically.

A3. Code Validation

Four code validation efforts were carried out over four different time periods in the life of the code. The first effort is described in considerable detail in Ref. 11. The code was successfully validated against analytical solutions and firing data

from the NASA Ames Research Center's 0.28"/1.55" and 1.5"/6.25" light gas guns. (The two numbers given identifying each gun are the lunch tube diameter and the pump tube diameter.) The comparisons are presented in some detail in Ref. 11.

The second code validation effort is described in Ref. 12. Forty-five shots with the Ames 0.5"/2.54" light gas gun were modelled with a version of the code which includes bore erosion and the incorporation of the eroded bore material into the hydrogen working gas. (The code used in the first code validation effort did not include bore erosion.) Muzzle velocities for these shots ranged from 4 to 9.5 km/s. The data included:

- (1) Projectile muzzle velocities
- (2) Piston velocities
- (3) Powder chamber maximum pressures
- (4) Bore erosion measurements

The code was successfully validated against the experimental data.

The third code validation effort is described in Ref. 14. In Ref. 14, experimental and CFD piston and muzzle velocities for the NASA Ames 0.22"/1.28", 0.28"/1.55", 0.50"/2.54", 1.00"/4.00" and 1.50"/6.25" guns are compared. Overall, the agreement between the experimental and CFD piston and muzzle velocities over the wide velocity range of 3 to 11 km/s was judged to be very good. It must be pointed out that, for muzzle velocities above 6 – 7 km/s, the gun code must take into account erosion of the steel gun tube wall material and the incorporation of it into the hydrogen working gas of the gun. This weighs down the working medium of the gun and leads to substantial reductions in muzzle velocity below those calculated without gun tube erosion.

The fourth code validation effort has not yet been presented in the literature but enters new territory and, hence, will be briefly described here. The objective in this study was to achieve low muzzle velocities (1 - 2.5 km/s). The guns used were the NASA Ames 0.30"/2.5" vertical gun (Ref. 15) and the NASA Marshall 0.22"/0.787" gun. In addition to shots with hydrogen working gas, shots were made with helium, nitrogen and argon working gases. Muzzle velocities of 0.7 - 5.7 km/s were successfully achieved, with the lower range of velocities (0.7 - 2.4 km/s) utilizing the heavy gases. These shots were modelled with the CFD code. The effects of changing the powder load and the working gas were well predicted by the code. The disagreements between experimental and CFD muzzle velocities were mostly in the range of 5 - 10%.

Additional validation of the LGGUN code is given in Secs. 3 and 6 of this report. Reference 16 is a detailed manual for LGGUN, describing its structure, subroutines, input and output files and other features and detailing how to put the code into action.

Appendix B - CFD Calculations and Experimental Data for Shots on the NASA Ames 0.28"/1.55" Gun with Short Pump Tube

In the series of 202 shots made with the NASA Ames 0.28"/1.55" gun from 8/25/66 to 7/29/68, the last 23 shots were made with a pump tube that was half the usual length. Several valuable observations were made during these "short pump tube" tests. These included:

- Measurements of the swelling of the small end bore of the HPC
- Observations of polyethylene piston material extruded into the barrel
- The effect of loading the projectile up to 30 cm down the barrel was noted

We first review seven of the shots for which CFD simulations were run. (These seven shots comprise a good cross section of the 23 "short pump tube" shots. Also, we note that a number of shots failed to provide adequate data due to break up of the projectile.) Table B1 (in two parts) gives key parameters for these shots. Note that, nominally, the firing conditions for shots 195 - 197 are the same, except for the placement of the projectile down the barrel. (The CFD code, at this time, does not have the ability to model a projectile placed some distance down the barrel.) The differences between the experimental and corresponding CFD piston and muzzle velocities are 1 to 4% for the piston velocities and 3 to 6% plus 1 each at 9% and 42% for the muzzle velocities. With the exception of the 42% value, these differences are in the same range or better as those found in the code validation reference (Ref. 14) for the NASA Ames 0.28"/1.55" gun with a full length pump tube.

For shot 197, the small end HPC bore swelled 0.008" (on a 0.300" bore).

For two of the four cases where the front of the piston was predicted by CFD to pass into the barrel (which starts at 549.5 cm), piston material was, in fact, found in the barrel. The fact that, in the remaining two cases, there is no notation in the log book of finding piston material in the barrel does not necessarily mean that there wasn't any - it just may not have been noted.

For shots 195 - 197, the muzzle velocity is observed to progressively drop as the projectile is loaded farther and farther down the barrel. However, since the experimental piston velocities are very nearly the same for shots 195 to 197, we assume that the CFD calculation for shot 196 (Fig. 10) also applies to shot 197, where the HPC swelling was observed experimentally. Thus, we can compare the experimental and CFD maximum pressures in the 0.300" bore of the HPC. The comparison is made in Section 7.

Table B1 (part 1). Key parameters for seven shots on the NASA Ames 0.28"/1.55" gun with short pump tube.

Shot number	Powder mass g	Hydrogen pressure psi	Piston velocity, exper. ft/s	Piston velocity, CFD ft/s	Percent difference between exp and CFD piston velocities
184	45	20.5	2459	2509	2.0
188	27	30.75	1905	1834	-3.7
194	45	30.75	2520.5	2491	-1.2
190	33	30.75	2155	2078	-3.6
195	39	20.5	2335.5	2313	-1.0
196	39	20.5	2355	2313	-1.8
197	39	20.5	2361	2313	-2.0

NASA Ames 0.28"/1.55" gun with half normal length pump tube

Projectile mass = ~0.162 g

Piston mass = 200 g

Powder mass = 27 to 45 g

Break valve rupture pressure = 10 ksi

HPC cone extends from x = 528.3 cm to x = 549.5 cm

Table B1 (part 2). Key parameters for seven shots on the NASA Ames 0.28"/1.55" gun with short pump tube.

Shot number	Projectile velocity, exper. km/s	Projectile velocity, CFD km/s	Percent difference between exp and CFD projectile velocities	Maximum x distance of piston front cm	Loading position of projectile down barrel cm	Polyethylene seen down barrel after shot	Comments regarding HPC
184	8.680	9.277	6.4	558.5	0		Outside dia. grew 0.002"
188	6.830	7.037	2.9	539.6	0		
194	8.467	8.938	5.3	545.3	0		
190	7.836	8.243	4.9	542	0		
195	8.808	9.214	4.4	552	10	Yes	0.300" hole grew 0.008"
196	8.348	9.214	9.4	552	20	Yes	
197	5.316	9.214	42.3	552	30		

Figures

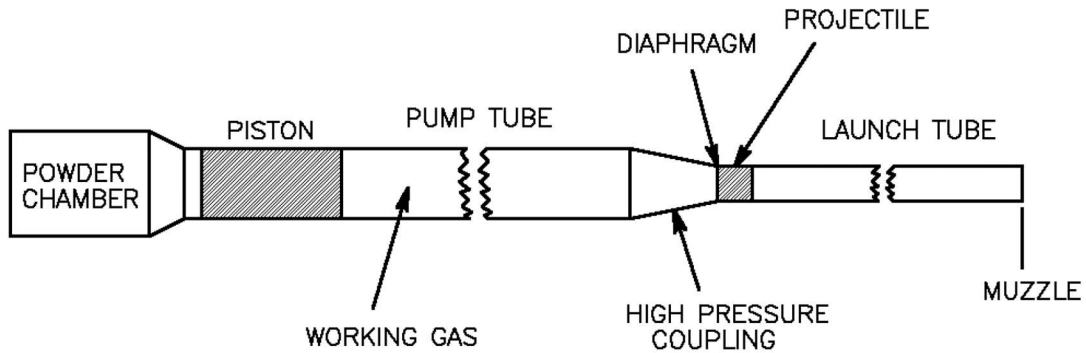


Figure 1. Schematic sketch of a two-stage light gas gun.
(This figure is also in the main text.)

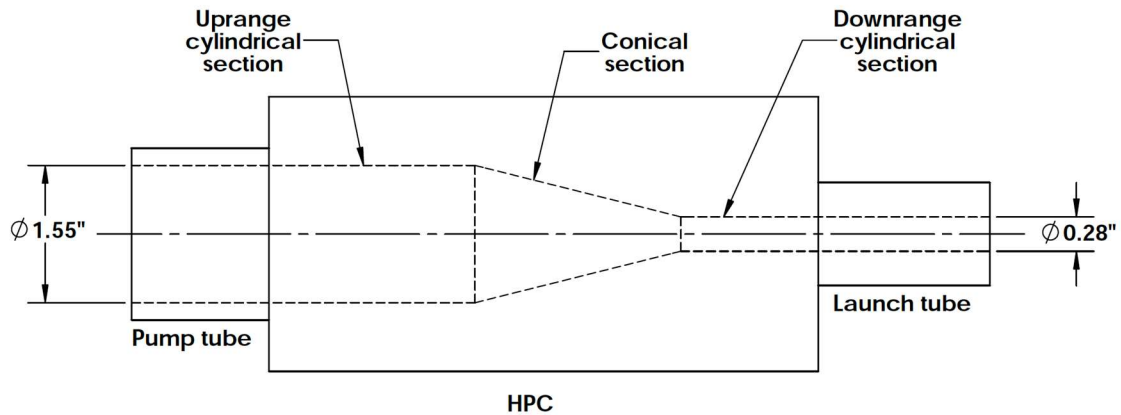


Figure 2. Sketch showing some details of the high pressure coupling (HPC) of a two-stage light gas gun. The dimensions shown are those for the NASA Ames 0.28"/1.55" gun.

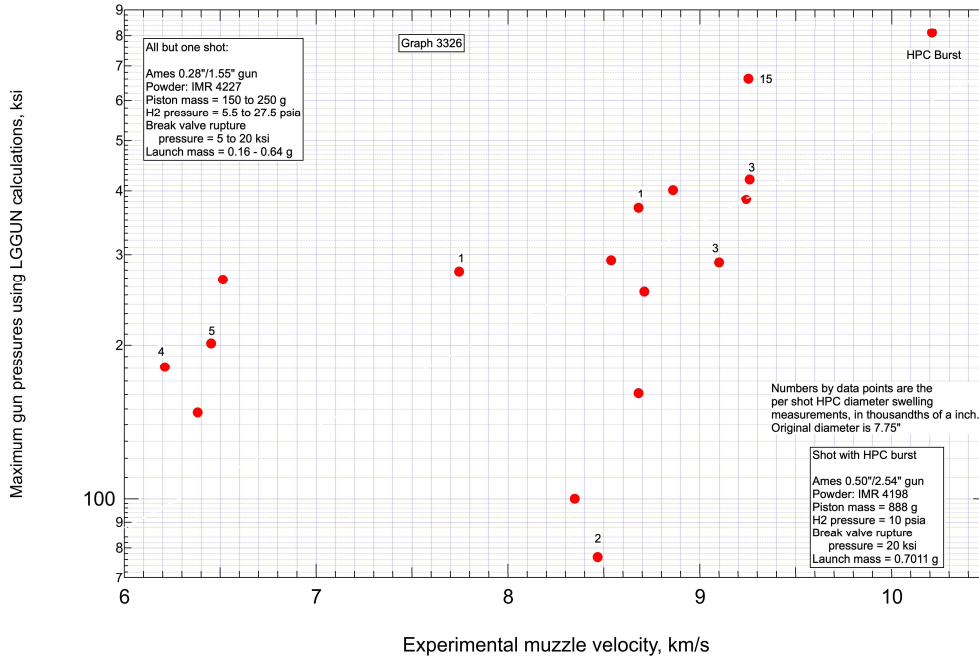


Fig. 3. Maximum gun pressures using LGGUN calculations versus muzzle velocity. (Note that the absence of numbers beside a data point does not mean that no swelling occurred for that shot, rather only that there is no swelling noted in the log book for that shot.)

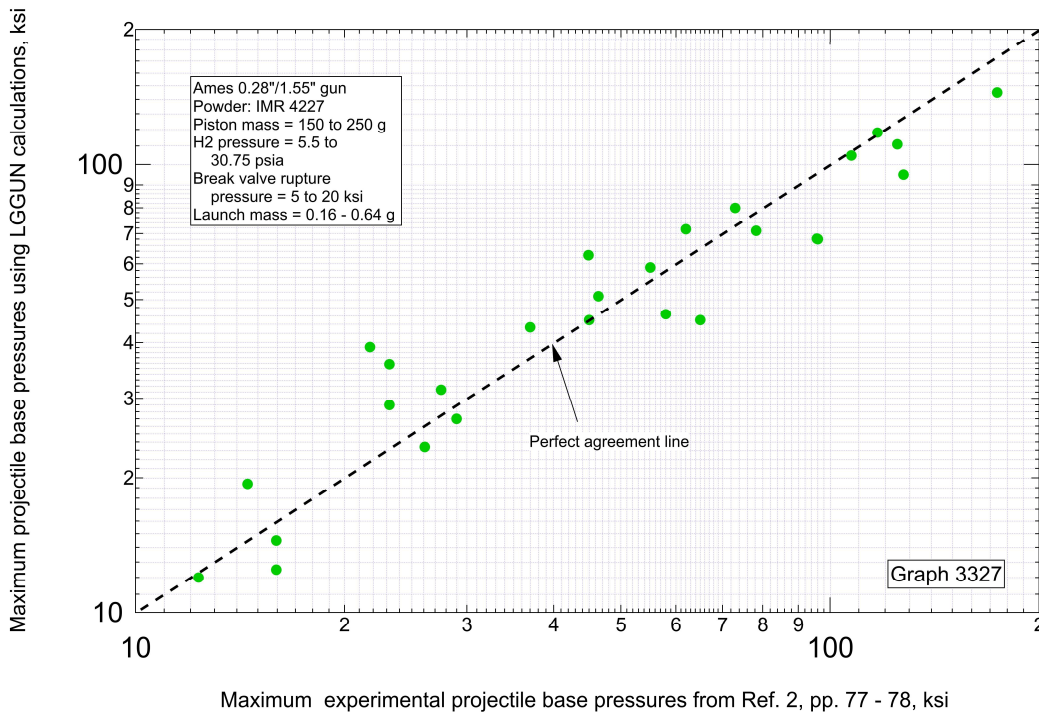


Fig. 4. Maximum projectile base pressures using LGGUN calculations and experimental results from Ref. 2.

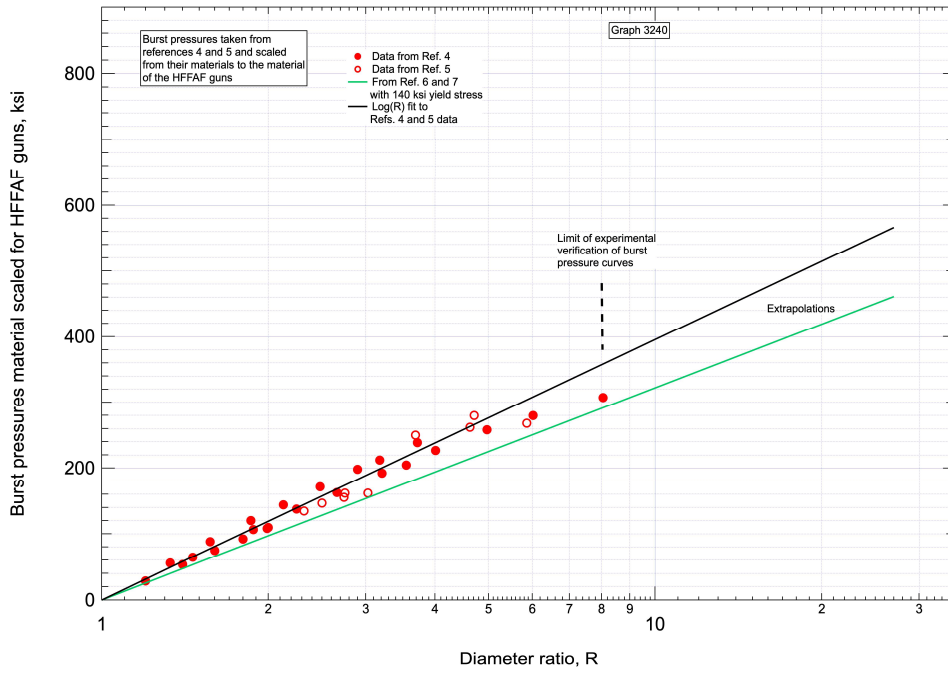


Fig. 5. Burst pressures material scaled for HFFAF guns versus diameter ratio.

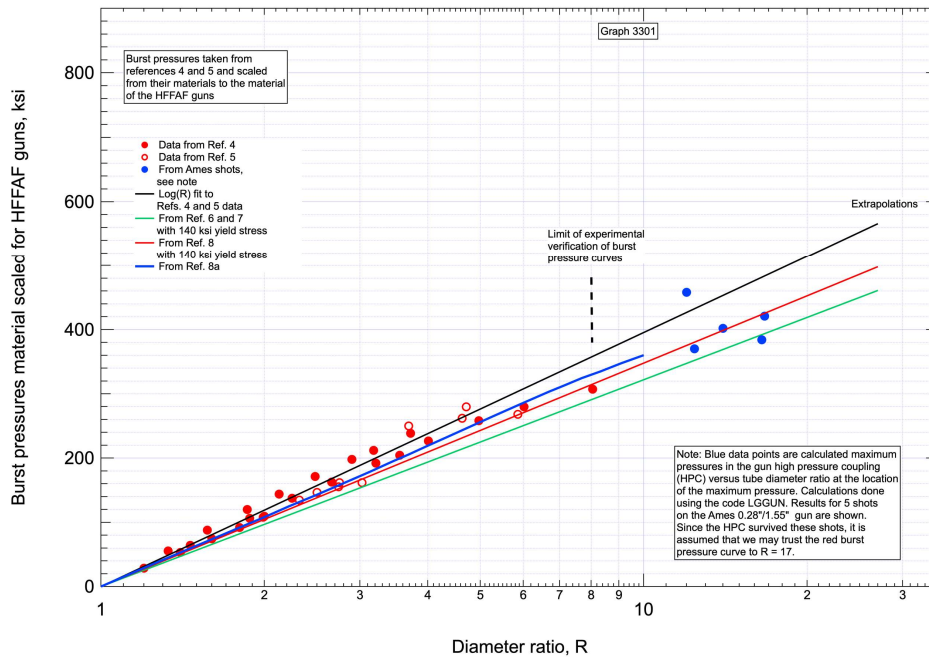


Fig. 6. Burst pressures material scaled for HFFAF guns versus diameter ratio (as in Fig. 5) with the addition of 5 new blue data points from the Ames 0.28"/1.55" gun and two new trend lines (red and blue).

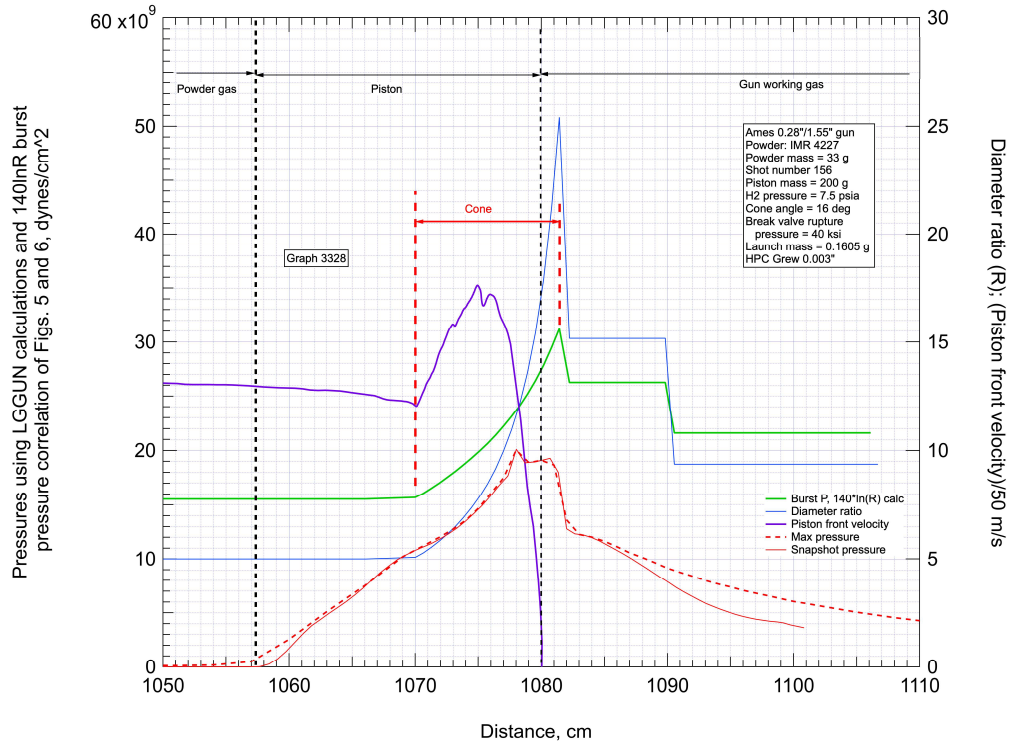


Fig. 7. Key outputs from the run of the CFD code LGGUN for shot 156 on the Ames 0.28"/1.55" two stage light gas gun.

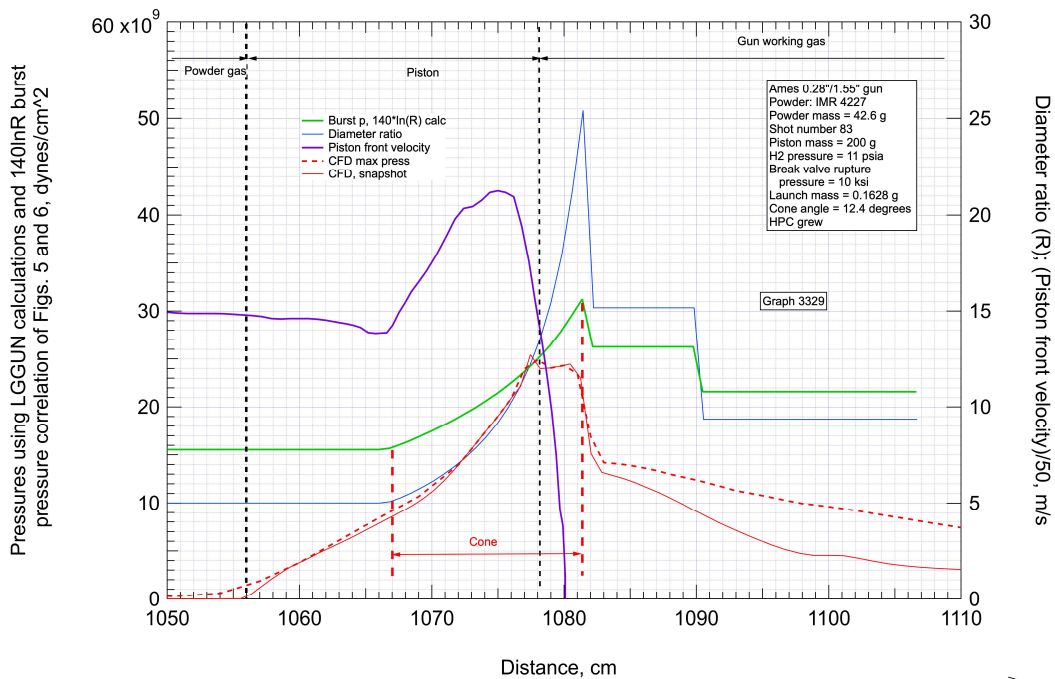


Fig. 8. Key outputs from the run of the CFD code LGGUN for shot 83 on the Ames 0.28"/1.55" two stage light gas gun.

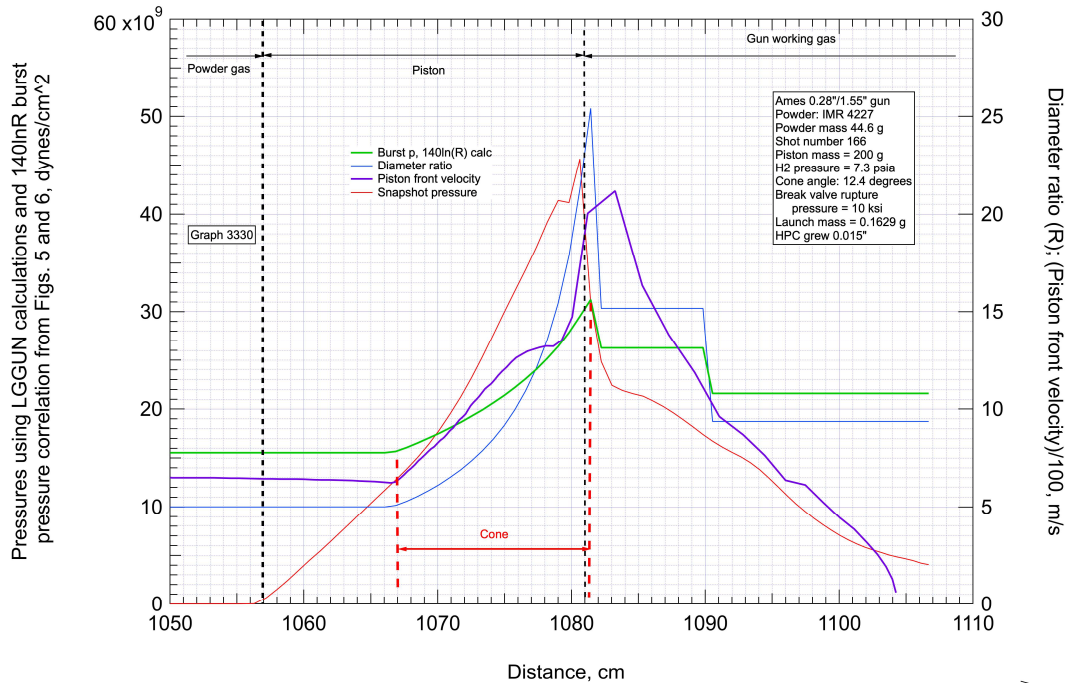


Fig. 9. Key outputs from the run of the CFD code LGGUN for shot 166 on the Ames 0.28"/1.55" two stage light gas gun.

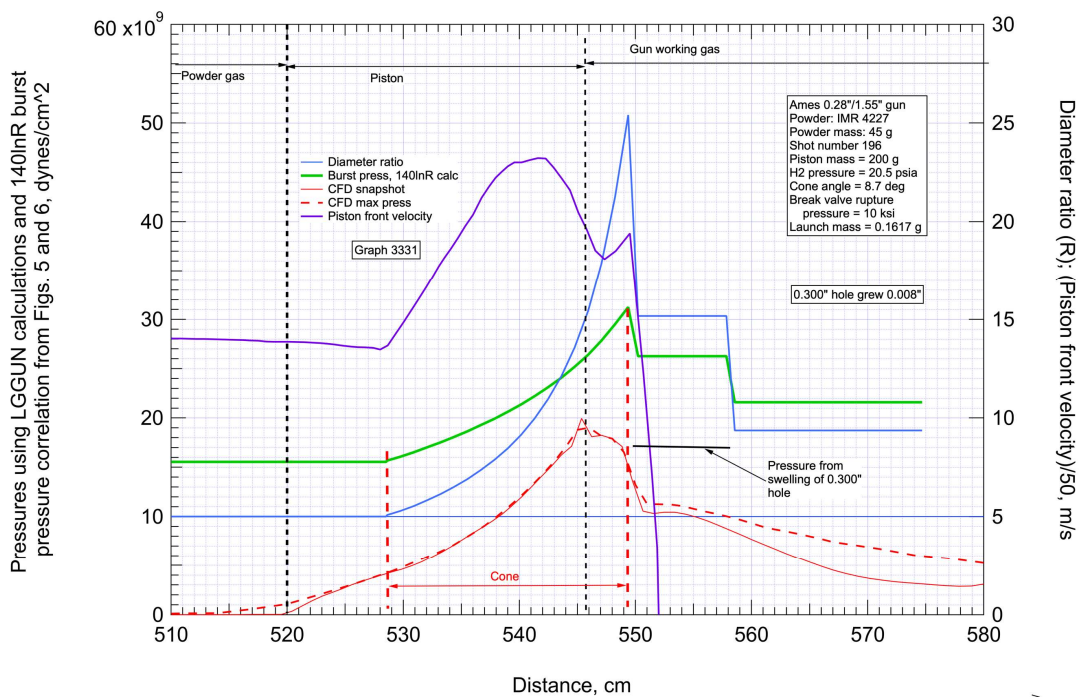


Fig. 10. Key outputs from the run of the CFD code LGGUN for shot 196 on the Ames 0.28"/1.55" two stage light gas gun.

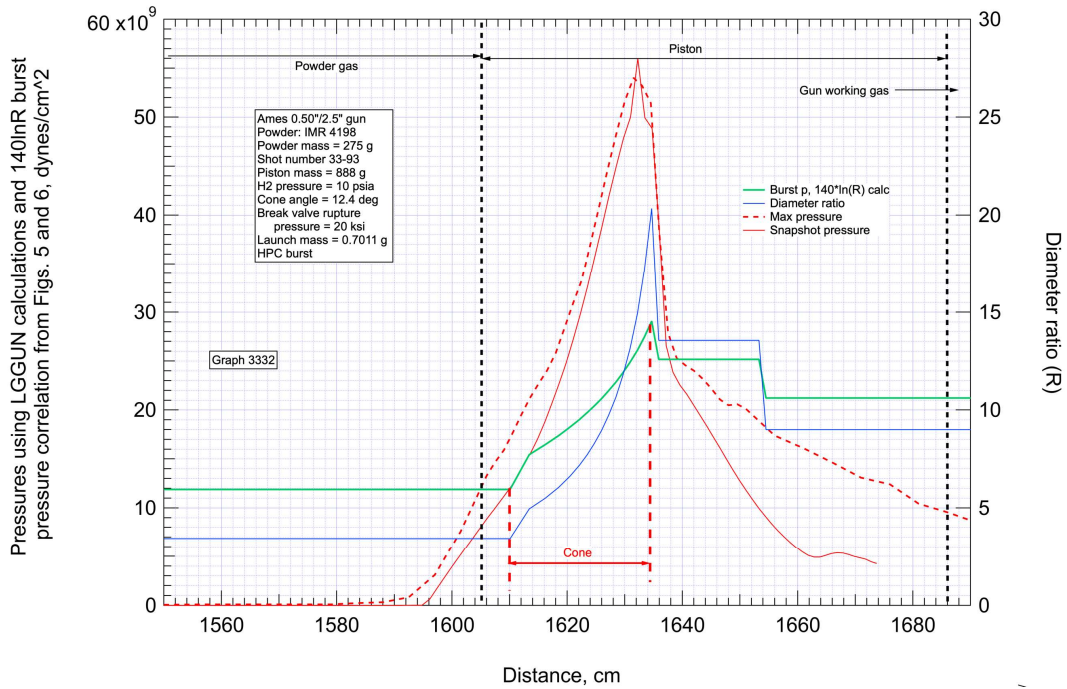


Fig. 11. Key outputs from the run of the CFD code LGGUN for shot 33 - 93 on the Ames 0.50"/2.50" two stage light gas gun.

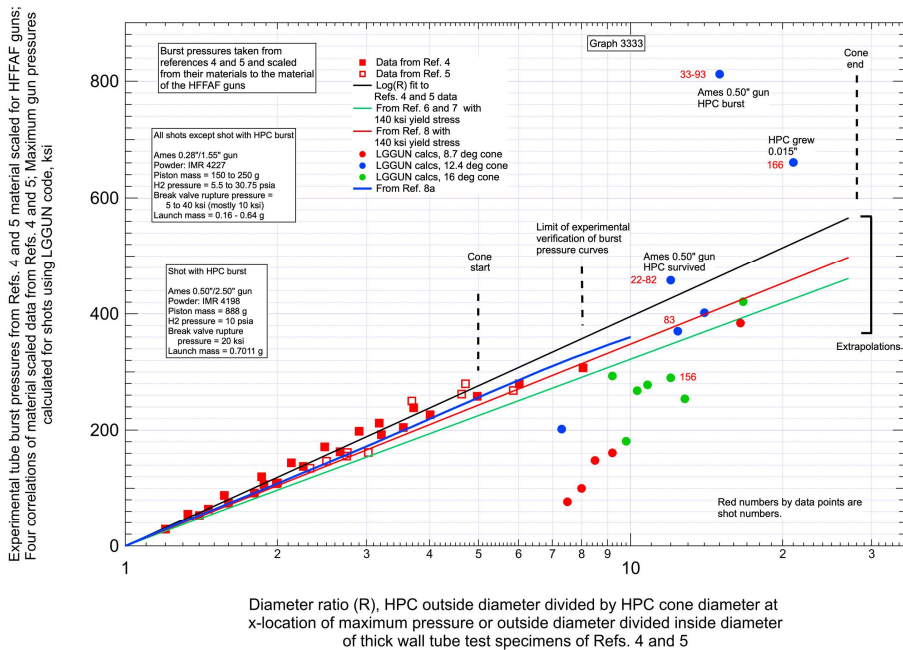


Fig. 12. Maximum gun pressures calculated for shots using LGGUN code and experimental tube burst pressures (data points and correlations) material scaled for HFFAF guns.

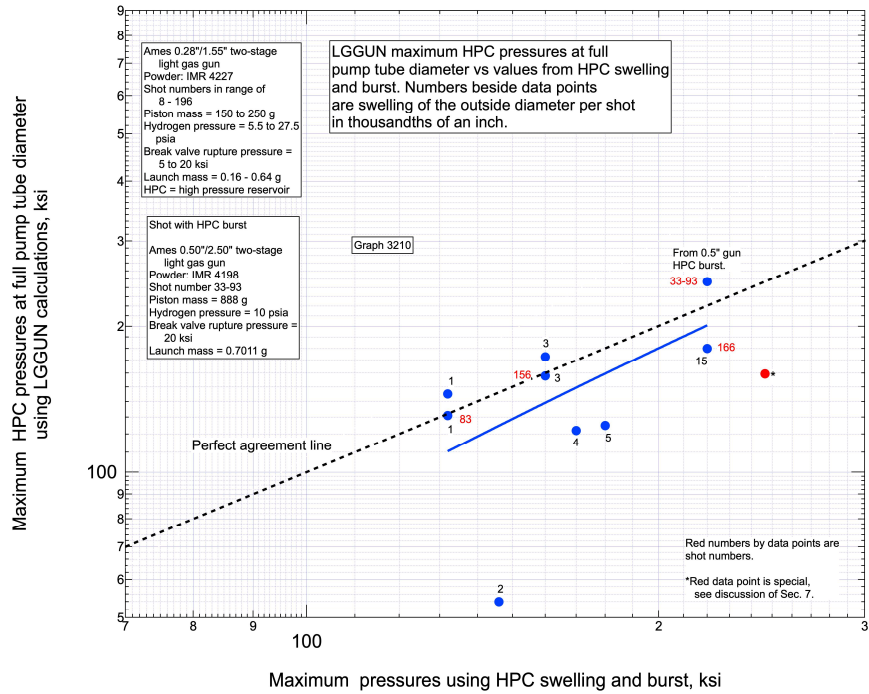


Fig. 13. LGGUN-calculated maximum HPC pressures in upstream cylindrical section of HPC vs values from HPC swelling and burst. Red data point is special, see discussion of Sec. 7.)

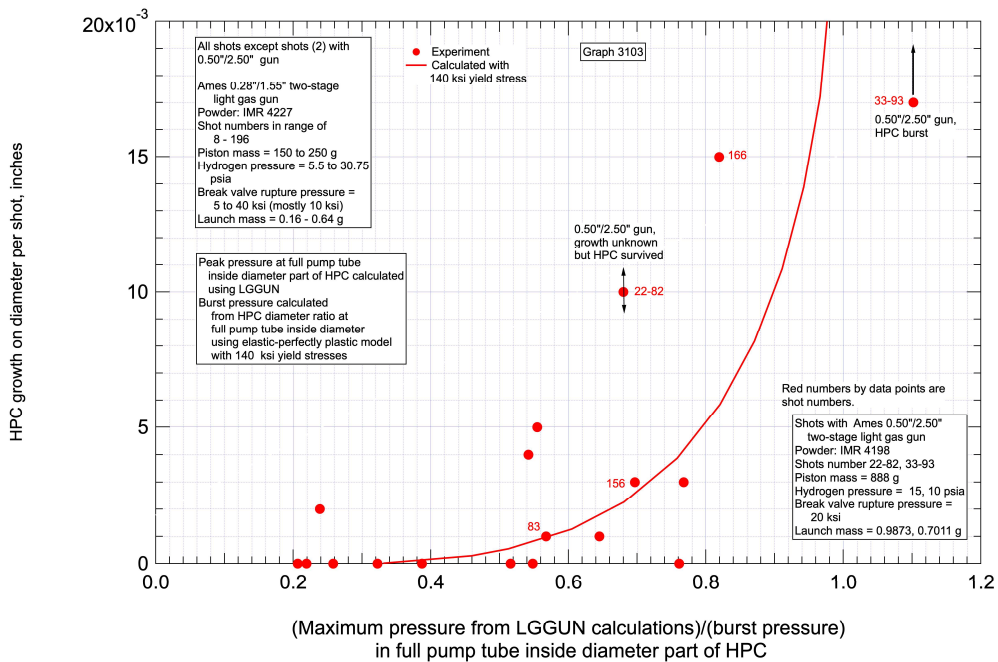


Fig. 14. (Maximum pressure from LGGUN calculations)/(burst pressure) in upstream cylindrical section of the HPC.

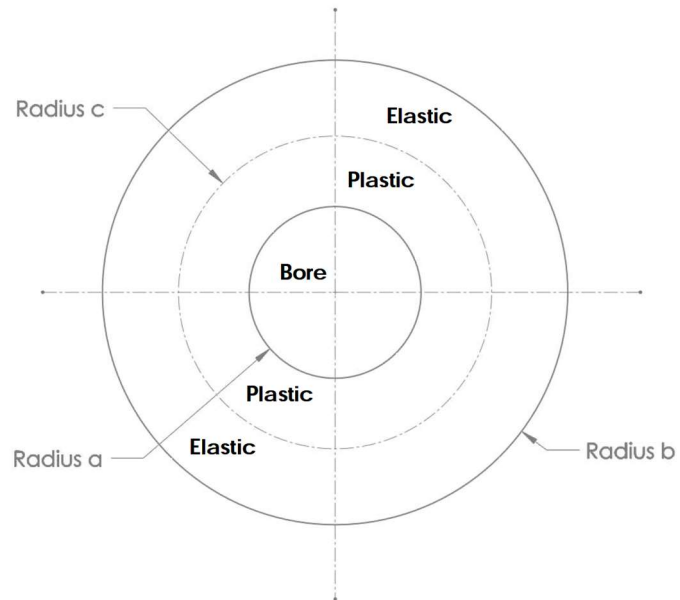


Fig. 15. Elastic and plastic zones and key radii for the elastic-plastic analysis of the HPC.

References

1. Log book "Gun Dev", NASA Ames HFFAF ballistic range, Bldg 237, 12/8/64 to 10/13/70.
2. Canning, T. N., Seiff, A. and James, C. S., "Ballistic Range Technology," AGARDograph 138, published by the North Atlantic Treaty Organization, Advisory Group for Aerospace Research and Development (AGARD), August, 1970.
3. *ibid*, Sec. 10.3.
4. Crossland, B. and Bones, J. A., "Behavior of Thick Walled Steel Cylinders Subjected to Internal Pressure", *Proc. Instn. of Mechanical Engineers*, Vol. 172, pp. 777-794, 1958.
5. Faupel, J. H., "Yielding and Bursting Characteristics of Heavy-Wall Cylinders," *Transactions of the ASME*, pp. 1033 - 1064, July 1956.
6. Popov, E. P., "Mechanics of Materials," 2nd ed., 1952, pp. 564 - 565.
7. Kelly, PA. *Mechanics Lecture Notes: An introduction to Solid Mechanics*, Section 8.5.4. available from <http://homepages.engineering.auckland.ac.nz/~pkel015/SolidMechanicsBooks/index.html>
8. Davidson, T. E. and Kendall, D. P., "The Design of Pressure Vessels for Very High Pressure Operation," Technical Report WVT- 6917, Benet R & D Laboratories, Watervliet Arsenal, Watervliet, New York, May 1963, pp. 19-43 (especially pp. 32 - 34 and Eq. 52).
- 8a. Crossland, B., Jorgensen, S. M. and Bones, J. A., "The Strength of Thick Walled Cylinders," *Journal of Engineering for Industry*, Transactions of the ASME, May, 1959, pp. 95 - 111.
9. Korsunsky, A. M., "Residual Elastic Strains in Autofrettaged Tubes: Elastic-Ideally Plastic Model Analysis," *Journal of Engineering Materials and Technology*, Vol. 129, January 2007, pp. 77 - 81.
- 9a. Popov, E. P., "Mechanics of Materials," 2nd ed., 1952, pp. 560 - 561, Eqs. (16-9) and (16-11).
10. Canning, T. N., Seiff, A. and James, C. S., *op. cit.*, pp. 11 - 95 and particularly, pp. 58, 82 and 83.
11. Bogdanoff, D. W. and Miller, R. J., "New Higher-Order Godunov Code for Modelling Performance of Two-Stage Light Gas Guns," NASA Technical Memorandum 110363, September, 1995.
12. Bogdanoff, D. W., "CFD Modelling of Bore Erosion in Two-Stage Light Gas Guns," NASA Technical Memorandum 1998-112236, August 1998.
13. MacCormack, R. W., "Current Status of Numerical Solutions of the Navier-Stokes Equations," AIAA Paper 85-0032, June 1985, p. 4.
14. Bogdanoff, D. W., "Further Validation of a CFD Code for Calculating the Performance of Two-Stage Light Gas Guns," NASA Technical Memorandum 2017-219571, September, 2017.
15. Site: [https://www.nasa.gov/sites/default/files/files/ames-vertical-gun-range-v2010\(1\).pdf](https://www.nasa.gov/sites/default/files/files/ames-vertical-gun-range-v2010(1).pdf).

16. Bogdanoff, D. W., "LGGUN User's Manual," NASA SP/2018-3714. December 2018.
17. Swift, H. F., Porter, C. D., Condon, J. J. and Baker, J. R., "NRL Hypervelocity Accelerator Development," Proceedings of the Sixth Symposium on Hypervelocity Impact, Cleveland, Ohio, April 30 to May 2, pp. 175 - 246.